International Journal of Mass Spectrometry 304 (2011) 115–123

Contents lists available at ScienceDirect

International Journal of Mass Spectrometry

journal homepage: www.elsevier.com/locate/ijms

Investigation of the reactivity of oligodeoxynucleotides with glyoxal and $KMnO_4$ chemical probes by electrospray ionization mass spectrometry

Carol Parr, Sarah E. Pierce, Suncerae I. Smith, Jennifer S. Brodbelt*

Department of Chemistry and Biochemistry, University of Texas at Austin, Austin, TX 78712, United States

ARTICLE INFO

Article history:
Received 18 March 2010
Received in revised form 6 June 2010
Accepted 7 June 2010
Available online 19 June 2010

Keywords:
Electrospray ionization
Chemical probe
Nucleic acid
Oligodeoxynucleotide
Glyoxal
Guanine

ABSTRACT

The reactions of two well-known chemical probes, glyoxal and potassium permanganate ($KMnO_4$), with oligodeoxynucleotides were monitored by electrospray ionization (ESI) mass spectrometry to evaluate the influence of the sequence of DNA, its secondary structure, and interactions with associated ligands on the reactivity of the two probes. Glyoxal, a guanine-reactive probe, incorporated a mass shift of 58 Da, and potassium permanganate ($KMnO_4$) is a thymine-reactive probe that resulted in a mass shift of 34 Da. The reactions depended on the accessibility of the nucleobases, and the peak abundances of the adducts in the ESI-mass spectra were used to quantify the extent of the chemical probe reactions. In this study, both mixed-base sequences were studied as well as control sequences in which one reactive site was located at the terminus or center of the oligodeoxynucleotide while the surrounding bases were a second, different nucleobase. In addition, the reactions of the chemical probes with non-covalent complexes formed between DNA and either actinomycin D or ethidium bromide, both known to interact with single strand DNA, were evaluated.

1. Introduction

The determination of DNA structure and conformation, ligand binding sites of DNA, as well as conformational changes caused by ligand binding, remains a formidable challenge. An array of traditional methods, including NMR, X-ray crystallography, circular dichroism, and gel electrophoresis have been used to examine the structures of DNA/ligand complexes [1–6]. The ligand binding mode and changes in DNA conformations can be determined using NMR [1] and X-ray crystallography [2,3], while the orientation of the bound ligand can be revealed using circular dichroism [4,5]. Footprinting analysis using gel electrophoresis, which has been the most popular analysis technique, reveals the location of the ligand as well as the identity of the DNA sequence [6]. However, these techniques often require a large amount of sample, can be time consuming, and, in the case of gel electrophoresis, do not always provide satisfactory resolution.

The use of chemical probes that react in a specific manner with DNA offers a versatile approach for obtaining specific information about DNA structures, ligand binding sites and potential conformational changes of DNA upon ligand binding [7–9]. These chemical probe methods rely on reactions that occur at selective DNA sites, most often involving nucleobases, and reveal whether specific sites are blocked or become more accessible upon ligand binding. A few of the more popular chemical probes that have been widely studied include osmium tetroxide (OsO_4) [10–12], dimethyl sulfate (DMS) [13,14], diethylpyrocarbonate (DEPC) [10,11,13–15], glyoxal [16–23], and potassium permanganate ($KMnO_4$) [7,8,24–26]. After reaction of the chemical probe with DNA, either in the absence or presence of an interactive ligand, the resulting products are typically analyzed by NMR or gel electrophoresis to assess the changes in reactivity and structure of the DNA upon ligand binding.

Recently, mass spectrometry has been used to monitor the products of reactions of nucleic acids with chemical probes [24,27–32], and this allows greater structural detail in characterization of the products in addition to providing quantitative information about the changes in nucleic acid reactivity upon ligand binding. Mass spectrometry has been applied in this way to analyze chemical probe reactions with DNA [24,27] and RNA [28–32]. For example, potassium permanganate ($KMnO_4$), a probe known to react with thymine, was used to study ligand binding to duplex DNA and determine the ligand binding sites along the duplex [24]. Reactions of glyoxal, a guanine-specific chemical probe, were used to determine the degree of conformational change caused by interaction of platinum-phenanthroimidazole complexes with the DNA quadruplexes [27]. Dimethyl sulfate (DMS), 1-cyclohexyl-3-(2-morpholinoethyl)carbodiimide methyl-*p*-toluenesulfonate (CMCT), and β-ethoxy-α-ketobutyraldehyde (kethoxal) were used by Kellersberger et al. to discriminate among single- and double-stranded regions of nucleic acids as well as obtain the footprint of bound proteins [28]. Additional studies also used the combination of DMS, CMCT, and kethoxal to evaluate

* Corresponding author. Tel.: +1 512 471 0028; fax: +1 512 471 8696.
E-mail address: jbrodbelt@mail.utexas.edu (J.S. Brodbelt).

1387-3806/$ – see front matter © 2010 Elsevier B.V. All rights reserved.
doi:10.1016/j.ijms.2010.06.007

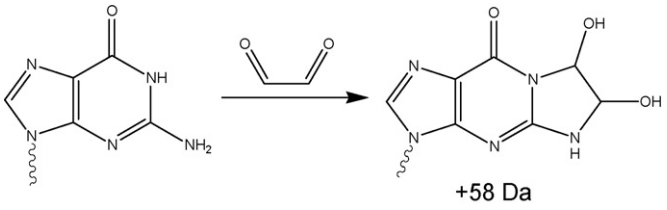

Scheme 1. Glyoxal reaction with guanine.

RNA structures including RNA-protein complexes and pseudoknots [29–31].

In the present study, we explore the use of ESI mass spectrometry to monitor the reactivity of two chemical probes, glyoxal and potassium permanganate ($KMnO_4$), with DNA to better understand the fundamental reactivity of these two chemical probes with DNA. The systematic nature of this study is aimed at elucidating the impact of the sequence of DNA, its secondary structure, and interactions with associated ligands as revealed by snapshots of the product distributions monitored by ESI-MS. Glyoxal is known to be endogenously formed by multiple cellular metabolic pathways [16,17] and can cause point mutations, deletions, and frame shift mutations [18–20]. Glyoxal reacts with guanine and to a lesser extent cytosine according to Scheme 1 in which the resulting product incorporates a mass shift of 58 Da [21] that can be easily monitored using mass spectrometry. Potassium permanganate ($KMnO_4$) has gained in popularity as a DNA chemical probe over the last few years because it reacts very specifically in the same manner as osmium tetroxide (OsO_4) yet posing far fewer hazards [25]. $KMnO_4$ has been shown to react with thymine and to a lesser extent adenine according to Scheme 2 [7,8,26]. The two resulting products are a diol with a mass shift of +34 Da and a α-hydroxylketone with a mass shift of +32 Da.

Exploiting the fact that these chemical probes react when the targeted nucleobase sites are accessible allows elucidation of the sites of DNA/ligand interactions based on mapping the reactivities of specific nucleobases in the absence and presence of DNA-interactive ligands that may block key sites. Products from the reactions of the chemical probes with DNA can be monitored based on new mass-shifted adducts that appear in the ESI-mass spectra, and the peak abundances of the adducts can be used to quantify the extent of the chemical probe reactions. Tandem mass spectrometry (MS/MS) can be used to determine the locations of the chemical probe adduction sites by careful interpretation of the fragmentation patterns (i.e. conventional a – B and w fragment ions will be mass shifted if they contain a chemical probe adduct). A prior study that evaluated the reactions of $KMnO_4$ with DNA showed that reactions occurred rapidly with single strand DNA because the permanganate had unobstructed access to the thymine bases; however, the reactivity of duplex DNA was greatly reduced because the native base-pairing limited the access of permanganate to the thymine bases [24]. Similarly, when a ligand was bound to the duplex DNA and thus unwound a portion of the double helix, the DNA reactivity increased due to the accessibility of certain nucleobases caused by the associated ligand [24]. The present systematic study focuses on the reactions of glyoxal and permanganate with single strand DNA and single strand DNA/ligand complexes.

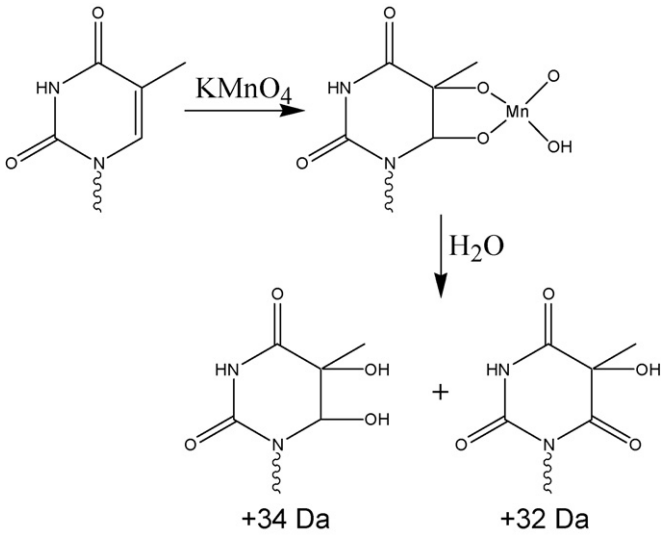

Scheme 2. Potassium permanganate reaction with thymine.

Table 1
Glyoxal reactivity.[a].

DNA sequence	# guanines	% reactivity	Net adduction value
SS1: 5′-AAAAAA**G**AAAAAAA-3′	1	12 ± 5	1.0
SS2: 5′-CCCCCC**G**CCCCCCC-3′	1	26 ± 9	1.2
SS3: 5′-TTTTTT**G**TTTTTTT-3′	1	13 ± 6	1.0
SS4: 5′-AAAA**G**AAA-3′	1	9 ± 4	1.0
SS5: 5′-**G**AAAAAAA-3′	1	55 ± 9	1.0
SS6: 5′-AAAAAAA**G**-3′	1	31 ± 5	1.0
SS7: 5′-**G**AAA**G**AAA-3′	2	45 ± 6	1.0
SS8: 5′-**GG**AAAAAA-3′	2	52 ± 6	1.1
SS9: 5′-AAA**GG**AAA-3′	2	19 ± 2	1.1
SS10: 5′-C**G**CCATATATCC**G**C-3′	2	77 ± 11	1.9
SS11: 5′-**G**CAAT**G**CCTAA**G**CC-3′	3	87 ± 10	2.1
SS12: 5′-**G**CGAT**G**CCTAC**G**CC-3′	4	84 ± 11	2.2
SS13: 5′-**GG**CTTA**GG**CATT**G**C-3′	5	89 ± 6	2.3
SS14: 5′-**G**CG**A**CG**C**C**G**A**C**G**C**C-3′	5	48 ± 12	1.5
SS15: 5′-**GG**CTA**G**CATC**G**C-3′	6	72 ± 16	1.7
SS16: 5′-C**GG**ATATAT**GG**C**G**-3′	6	78 ± 14	2.0
SS17: 5′-**GCGCGCG**CTAAAAA-3′	4	69 ± 9	1.8
SS18: 5′-**GCGCGCG**CAAAAAT-3′	4	68 ± 7	1.7
DS1: 5′-**GCGG**ATATAT**GGCG**-3′ 3′-C**G**CCTATATACC**G**C-5′	8	14 ± 7	1.2
DS2: 5′-**GGCG**TC**GGCG**TC**G**C-3′ 3′-CC**G**CA**G**CC**G**CA**G**C**G**-5′	12	28 ± 10	1.1
DS3: 5′-**GG**CTTA**G**CATT**G**C-3′ 3′-CC**G**AATCC**G**TAAC**G**-5′	8	32 ± 11	1.2

[a] The percent reactivities are determined for solutions containing a DNA single strand (40 μM in 50 μL of 90 mM ammonium acetate) incubated with 1 μL of an aqueous 20% glyoxal solution for 30 min at 37 °C. The percent reactivity value is a measure of the extent of the glyoxal adduction to the selected DNA (see equation in Section 2) based on relative abundances of adducted and non-reacted DNA ions. The net adduction value is a measure of the average number of additions of glyoxal to the selected DNA (see equation in Section 2). All guanines are highlighted in bold font.

2. Experimental

2.1. Materials

Single strand oligodeoxynucleotides were purchased from Integrated DNA Technologies (Coralville, IA) and synthesized on the 1 μmole scale and desalted by a proprietary technique similar to using an oligodeoxynucleotide purified column (OPC) method. The sequences used in this work and their abbreviated names appear in Table 1. Actinomycin D, ethidium bromide, and $KMnO_4$ were purchased from Thermo Fisher Scientific (Waltham, MA) and used without further purification. Glyoxal was purchased from Acros Organics (Morris Plains, NJ) and used without further purification. All solvents were of HPLC grade purity.

2.2. Chemical probe reactions

Prior to the chemical probe reactions, stock solutions of each single strand oligodeoxynucleotide were prepared at approximately

1 mM in water, and the exact concentration was determined based on UV–Vis absorbance measurements at 260 nm. Stock solutions of actinomycin D and ethidium bromide were prepared at 1 mM in methanol.

Solutions containing a DNA single strand were prepared at 40 μM in 50 μL of 90 mM ammonium acetate. Where indicated, a ligand was added at 120 μM and the solution was allowed to equilibrate for at least 30 min at room temperature. To initiate the glyoxal reaction, 1 μL of an aqueous 20% glyoxal solution was added to the DNA/ligand solutions and the reaction mixture was incubated for 30 min at 37 °C. For the $KMnO_4$ reactions, 5 μL of an aqueous 5 mM $KMnO_4$ solution was added to the DNA solution and allowed to react at room temperature for 30 min. After the incubation, unreacted glyoxal or $KMnO_4$ was immediately removed from the solution using a Pierce PepClean C_{18} spin column (Rockford, IL). The DNA was eluted from the column using 40 μL of 50% acetonitrile solution and then diluted to 100 μL so that the final solution was approximately 16 μM DNA in 50 mM ammonium acetate.

2.3. Mass spectrometry

Analytical solutions were directly infused into a ThermoFinnigan LCQ Duo mass spectrometer (San Jose, CA) at 3 μL/min using a Harvard Apparatus PHD 2000 syringe pump (Holliston, MA). Negative ions were produced using an ESI voltage of 3.5 kV and a heated capillary temperature of 90 °C. Nitrogen sheath and auxiliary gas flows of 40 and 10 arbitrary units, respectively, were used to aid the desolvation of the ions. The base pressure of the trap was nominally 1×10^{-5} T. The percent reactivity value, which is a semi-quantitative means of assessing the extent of reaction of each chemical probe with each DNA sequence, was calculated using the following formula.

$$\%\ \text{Reactivity} = \frac{H_{[M+A]} + 2H_{[M+2xA]} + \cdots nH_{[M+nxA]} \times 100\%}{H_{[M]} + H_{[M+A]} + 2H_{[M+2xA]} + \cdots nH_{[M+nxA]}} \quad (1)$$

where $H_{[M]}$ is the peak height for the unreacted DNA and $nH_{[M+nA]}$ is the peak height of the nth adducted product. The complexes containing more than one adduct are weighted more heavily to reflect the greater extent of reactivity. Additionally, the net adduction value was also calculated using the following equation.

$$\text{Net Adduction Value} = \frac{H_{[M+A]} + 2H_{[M+2A]} + nH_{[M+nA]}}{H_{[M+A]} + H_{[M+2A]} + H_{[M+nA]}} \quad (2)$$

This gives a representation of the average number of adducts observed for a particular oligodeoxynucleotide. The net adduction values were calculated for each of the charge states seen in the spectra and then all the values were averaged together for a given sequence.

3. Results and discussion

In this study, numerous experiments were carried out to further understand glyoxal reactions with single strand DNA. Both mixed-base sequences were studied as well as two sets of "control sequences". For one set of control sequences, one reactive site is located at the center of the oligodeoxynucleotide while the surrounding bases are a second, different nucleobase. This allowed the effect of neighboring bases to be evaluated for each of the reactions as well as to determine if secondary reactions also occur at other nucleobases. The second set of control sequences were adenine-rich sequences containing a single or two guanine nucleobases in order to evaluate the impact of the position of the guanine sites on reactivity with glyoxal. Additionally, the reactions of the chemical probes with non-covalent complexes formed between DNA and either actinomycin D or ethidium bromide, both known to interact with single strand DNA, were studied. It was expected that the reactivity of the DNA/ligand complexes would be lower than that of the native single strands because the ligands should block some of the reactive sites. Moreover, a decrease in reactivity as more ligands are bound to the DNA is anticipated because more nucleobases become inaccessible. Some comparisons of reactivity were also undertaken using potassium permanganate ($KMnO_4$), another chemical probe studied previously in our lab [24].

3.1. Glyoxal reactivity with DNA

The first experiments were undertaken by examining the reactivity of glyoxal with oligonucleotides in which only one reactive nucleobase was present. An example of the distribution of products arising for dAAAAAAAG after a 30 min reaction period with glyoxal at 37 °C is shown in Fig. 1. (Another example is shown in Supplemental Fig. 1 for the reactions of glyoxal with a longer oligodeoxynucleotide, d(GCGGATATATGGCG)). The key product ions of interest have a net mass shift of +58 Da indicative of glyoxal adduction and are labeled accordingly with the number of glyoxal adducts indicated in parenthesis. The 58 Da mass shift is sufficiently large that the glyoxal adducts are easily distinguishable from the sodium adducts. One glyoxal adduct is observed for each of the two charge states of dAAAAAAAG. The percent reactivity value was calculated from the abundances of the non-adducted DNA and the glyoxal adducts according to Eq. (1) in order to provide a semi-quantitative comparative means of evaluating the extent of reaction for DNA sequence. For dAAAAAAAG, the reactivity value was 31% with a 5% standard deviation based on three replicates, and the net adduction value was 1.0. The percent reactivity values for the reactions of glyoxal with an array of other sequences are summarized in Table 1, as discussed below.

Reactions of glyoxal with a series of 14-mer oligodeoxynucleotides containing a single guanine base located in the middle of the strand and surrounded by continuous stretches of a second nucleobase i.e. d(AAAAAAGAAAAAAA) (SS1) were undertaken. (see Table 1) Relatively lower reactivity was seen for the adenine-rich (SS1) and thymine-rich (SS3) sequences compared to the cytosine-rich strand (SS2). This suggests that neighboring cytosine residues either influence the reactivity of glyoxal with guanine or glyoxal reacts with the cytosine residues as well as the guanine. Because multiple adducts are seen in the spectrum for this latter reaction (as evidenced in Table 1 by the slightly higher adduction value for the C-rich oligodeoxynucleotide SS2 (1.2) relative to the other two single strands, SS1 and SS3), there is evidence supporting some reactivity at cytosine residues, but it cannot be said conclusively if this is the only factor contributing to the higher reactivity observed. Due to the potential cross-reactivity of glyoxal with cytosine, the reaction of glyoxal with d(CCCCCC) was also evaluated, and it was found that this strand exhibited low reactivity with glyoxal, with a percent reactivity of 15%. This non-zero percent reactivity confirms that glyoxal has the potential to react with cytosine, albeit with low efficiency.

The effect of the duration of the treatment with glyoxal was examined using the single strand d(GCGACGCCGACGCC) (SS14) which contains five possible reactive sites (guanines) to encourage higher reactivity. In previous reports (ones not utilizing mass spectrometry to follow the reaction products), reaction times from 5 min to seven days were used with little justification [17,22,23], and thus the reactions were monitored over a range of times by ESI-MS in the present study to illustrate that the reaction time plays a significant role and must be carefully controlled. Fig. 2a shows the ESI-mass spectrum of a solution containing the single strand after 30 min of reaction with glyoxal. The spectral region around $[ss]^{-4}$ (m/z 1050–1300) is shown in the inset and multiple glyoxal adducts as well as low abundance sodium adducts that are labeled with an

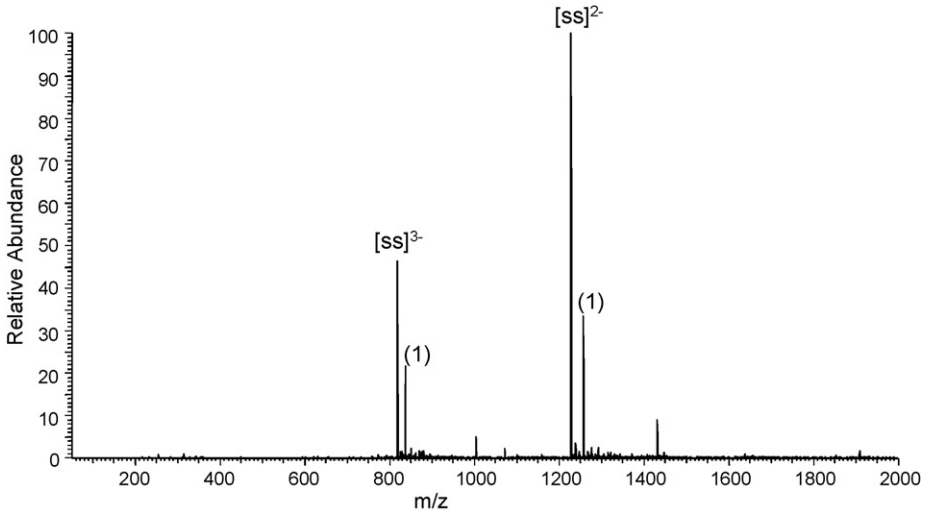

Fig. 1. ESI-mass spectrum showing the single strand d(AAAAAAAG) (SS6) after 30 min reaction with glyoxal at 37 C. Ions containing a glyoxal addition are labeled with a number in parenthesis indicating the number of glyoxal adducts.

asterisk (*) are detected. The corresponding spectrum of the same single strand after 60 min reaction with glyoxal is shown in Fig. 2b. Five guanine sites are theoretically accessible for glyoxal reactions, in agreement with the results observed after 60 min and with the collective products nearly as abundant as the unreacted single strand. After 10 h reaction with glyoxal, the glyoxal adducts are far more abundant than the un-adducted single strand as illustrated in Fig. 2c. Following such a lengthy reaction period, the spectrum is too cluttered to be accurately analyzed or to discern glyoxal adducts from sodium adducts, a drawback of the ESI-MS approach relative to gel-based analysis. From these data, 30 min was chosen as a sufficient reaction time to show abundant adducts that are clearly seen but that do not suppress or over-shadow detection of the unreacted single strand species. Additionally, a shorter reaction time was preferred in order to increase sample processing. Experimental results acquired at a specific reaction time (i.e. typically 30 min for the present study) give a snapshot of the DNA/chemical probe reactivities and are meant to facilitate systematic comparisons among different DNA sequences, not to imply that the reactions have gone to completion.

The position of the guanine(s) within the oligodeoxynucleotide sequence was probed to examine the impact of the location of the guanines on glyoxal reactivity. For this study, a series of 8-mer oligodeoxynucleotides were chosen with either one or two guanine bases at different sites in the sequence, and these are listed in Table 1 as SS4–SS9. The first three sequences (SS4–SS6) each contain one guanine, and the location of this reactive site exhibits a substantial impact on the resulting reactivity. The reactivity of the oligodeoxynucleotide containing the guanine in the center of the sequence (SS4) is much lower than when the guanine is located on one of the termini (SS5 and SS6). Additionally, greater reactivity is observed when the guanine base is located on the 5′ end of the oligodeoxynucleotide. This trend is generally maintained when two guanines are located next to each other as observed for oligodeoxynucleotides SS8 and SS9 in which the former exhibits a significantly higher reactivity (52%) compared to the latter (19%).

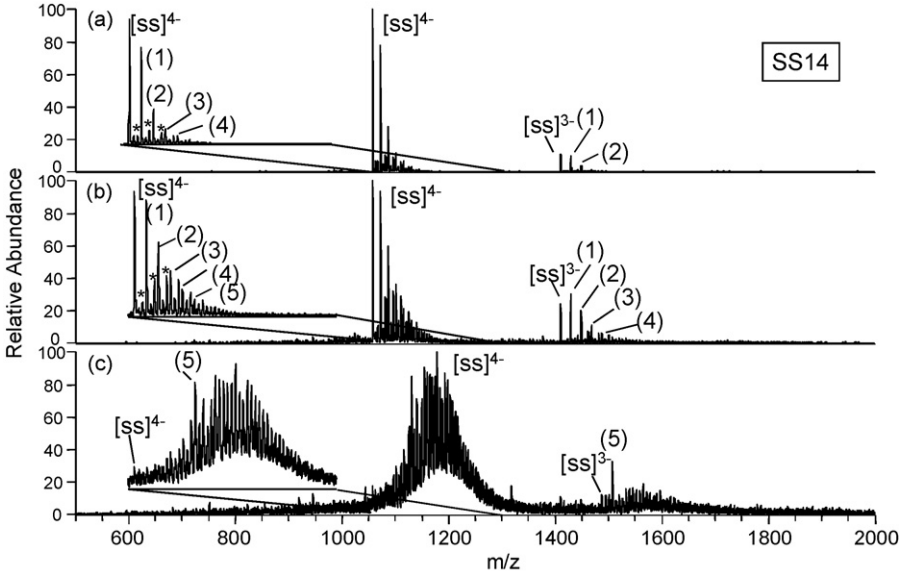

Fig. 2. ESI-mass spectra showing the single strand d(GCGACGCCGACGCC) (SS14) (a) after 30 min reaction with glyoxal, (b) after 60 min reaction with glyoxal, and (c) after 10 h reaction with glyoxal all at 37 C. Spectral enlargements of the region around *m*/*z* 1050–1300 are shown in the inset. Ions containing a glyoxal addition are labeled with a number in parenthesis indicating the number of glyoxal adducts. Ions labeled with * correspond to sodium adducts.

Although the underlying reasons are unclear, reactions at terminal guanine residues appear to be more favorable and/or more efficient than reactions at interior guanine residues. Along those same lines, the reactivity of SS7, which contains one guanine at a terminal position and one at an interior position, displays intermediate reactivity between SS8 and SS9. This result suggests that glyoxal may react at either of the two guanine sites, with reaction at the interior guanine contributing to the lower reactivity compared to SS8. Moreover, the fact that the net adduction values for all of these six 8-mers are close to 1.0 indicates that the multiple adduction of glyoxal is not a significant pathway under these experimental conditions.

To further map the reactivity of glyoxal with single strands, a variety of other oligodeoxynucleotides (SS10–SS18) were chosen to vary the number and location of the guanine residues in the sequences. Each of these sequences was allowed to react with glyoxal for 30 min, and the percent reactivities and net adduction values are summarized in Table 1. Upon examination of the results in Table 1, the reactivity values consistently fall in the range of 70–90% (except for SS14) without a strong correlation with the specific number or location of the guanine residues in the sequence. The net adduction values lie in the range of 1.7–2.3 for most of the sequences (aside from the lower value for SS14), and these adduction values correlate with the reactivity values. Since the adduction value conveys the average number of adducts detected for a particular oligodeoxynucleotide, a value close to two indicates that most of the products incorporate the addition of two glyoxal moieties regardless of the number of guanines in the 14-mer sequences. As shown from the results in Table 1, the generally high reactivity of glyoxal with single strand oligodeoxynucleotides containing two or more guanines suggests that ESI-MS can be readily used to monitor guanine accessibility.

The reactivity and adduction value of SS14 is lower than the other 14-mer sequences. This particular sequence is the most GC-rich sequence, and we speculate that its lower reactivity may arise from its potential to form a partial stem–loop structure via base-pairing of the GCG and CGC segments. Formation of a structure with intramolecular interactions could inhibit the accessibility of glyoxal in solution, a factor responsible for the reduced reactivity of duplexes, as discussed below. It is difficult to confirm the formation and survival of partial hairpin or other secondary structures for the 14-mer sequences shown in Table 1, especially given the conditions required for optimization of the glyoxal reactions (addition of an aqueous 20% glyoxal solution to the DNA and incubation for 30 min at 37 °C). Nondenaturing gel determination of the migration profiles of four of the strands shown in Table 1 (SS10, SS12, SS14, and SS15) indicated that the latter three adopted at least partial hairpin conformations, whereas SS10 did not. While this result is generally consistent with the prediction of partial hairpin secondary structures based on statistical mechanics calculations [33,34], it does not completely explain the low reactivity of SS14 relative to SS12 and SS15 (all predicted to adopt relatively weak partial hairpin structures) and could point to other factors that modulate glyoxal reactivity, such as the location of the guanine residues in the stem or loop segments, the relative distribution of different secondary structures, or the impact of other specific nucleotides in the sequences.

The reactivity of glyoxal with duplex DNA was investigated to examine the impact of base-pairing, a factor which presumably should reduce accessibility of the reactive sites of the guanines. For this series of experiments, the reactivities were examined individually for each of the two complementary single strands as well as the corresponding duplex. An example of this comparative strategy is shown in Fig. 3 for SS16, SS10, and the corresponding duplex. As anticipated based on the results discussed above for single strand oligodeoxynucleotides, the reactivity values obtained from the spectra in Fig. 3a and b are high, averaging around 75%. In contrast the reactivity for the duplex is only 28%, indicating a significant suppression due to base-pairing. Additionally, the low reactivity observed for the low abundance single strand species present in Fig. 3c indicates that these single strands likely arise from disassembly of the duplexes after the glyoxal reaction, not from native single strands. In fact, the ESI-mass spectrum of DS1 prior to the reactions with glyoxal displays virtually no single strand species, but some disruption of the duplexes occurs during the glyoxal reactions and subsequent clean-up. This means that the level of glyoxal adduction for the observed single strand species in Fig. 3c is comparable to the reactivity of the duplex, not to the reactivity of the free single strands seen in Fig. 3a and b. The calculated reactivity values for duplex DS1 and two others are shown in the bottom section of Table 1. While extensive reactivity is observed for each of the single strands, the three duplexes exhibit considerable lower reactivity, averaging 30%. The net adduction values (1.1–1.2) of the duplexes are likewise lower than the adduction values observed for the single strands, again indicating a reduction in guanine accessibility.

Table 2
$KMnO_4$ reactivity.[a]

DNA sequence	# thymines	% reactivity	Net adduction value
SS17: 5′-GCGCGCGC**T**AAAAA-3′	1	63 ± 5	1.1
SS18: 5′-GCGCGCGCAAAAA**T**-3′	1	66 ± 4	1.1
SS19: 5′-AAAAAA**T**AAAAAAA-3′	1	56 ± 13	1.1
SS20: 5′-CCCCCC**T**CCCCCCC-3′	1	62 ± 9	1.2
SS12: 5′-GCGA**T**GCC**T**ACGCC-3′	2	88 ± 8	1.6
SS15: 5′-GGCG**T**AGGCA**T**CGC-3′	2	83 ± 9	1.5
SS10: 5′-CGCCA**T**A**T**A**T**CCGC-3′	3	96 ± 2	2.6
SS13: 5′-GGC**TT**AGGCA**TT**GC-3′	4	96 ± 3	3.1

[a] The percent reactivities are determined for solutions containing a DNA single strand (40 μM in 50 μL of 90 mM ammonium acetate) incubated with 5 μL of an aqueous 5 mM $KMnO_4$ solution for 30 min at room temperature. The percent reactivity value is a measure of the extent of oxidation of the selected DNA (see equation in Section 2) based on relative abundances of oxidized and non-oxidized DNA ions. The net adduction value is a measure of the average number of oxidations of selected DNA (see equation in Section 2). Thymines are highlighted in bold font.

3.2. $KMnO_4$ reactivity with DNA

The reactivity of single strand oligodeoxynucleotides with potassium permanganate ($KMnO_4$) was also investigated. We have studied the reactions of potassium permanganate with duplex DNA and duplex/ligand complexes previously [24]. These efficient, base-selective reactions were readily monitored by ESI-MS and suggested that this chemical probe would also be useful for investigations of single strand/ligand complexes. As with the glyoxal reactions, a standard reaction time of 30 min was utilized for the $KMnO_4$ reactions to ensure adequate and reproducible product distributions. As an example, Fig. 4 shows the product distributions obtained upon reaction of $KMnO_4$ with a representative oligodeoxynucleotide, d(GGCGTAGGCATCGC) (SS15). Oxidized products are labeled with the number of adducts indicated in parenthesis. This sequence exhibits substantial reactivity (83%), as seen by the large adduct peaks in Fig. 4, with up to three adduction sites. The results obtained upon the oxidation of an array of other oligodeoxynucleotide sequences are summarized in Table 2. In general, the reactivity of $KMnO_4$ increases with the number of thymine residues, and the number of adduction sites is greater than observed for the glyoxal reactions for sequences containing comparable numbers of thymine (for $KMnO_4$ reactions) or guanine (for glyoxal) nucleobases.

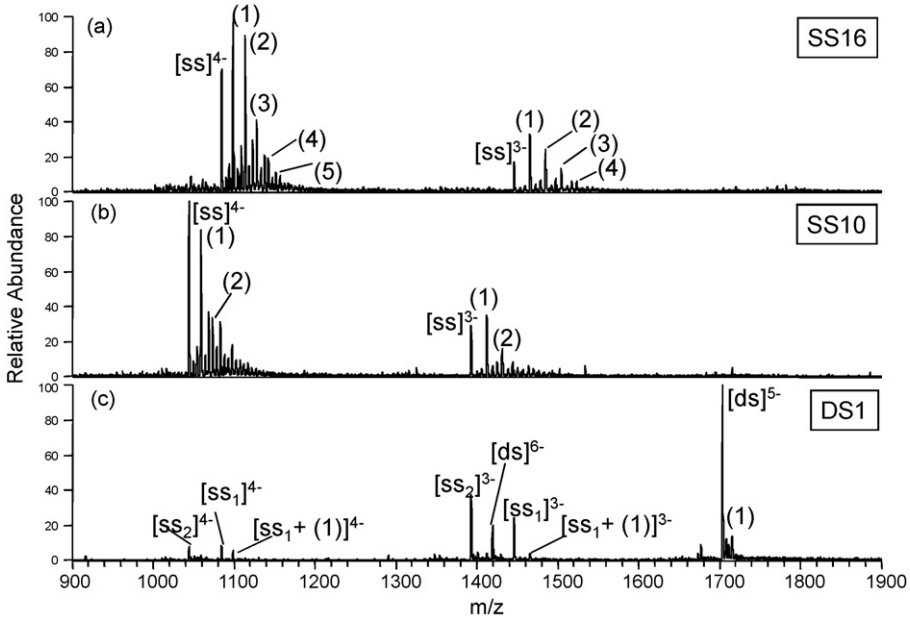

Fig. 3. ESI-mass spectrum showing glyoxal reactivity with (a) d(GCGGATATATGGCG) (SS16), (b) d(CGCCATATATCCGC) (SS10) and (c) the respective duplex d(GCGGATATATGGCG/CGCCATATATCCGC) (DS1). An ion retaining a glyoxal adduct is labeled with the number of adducts indicated in parenthesis.

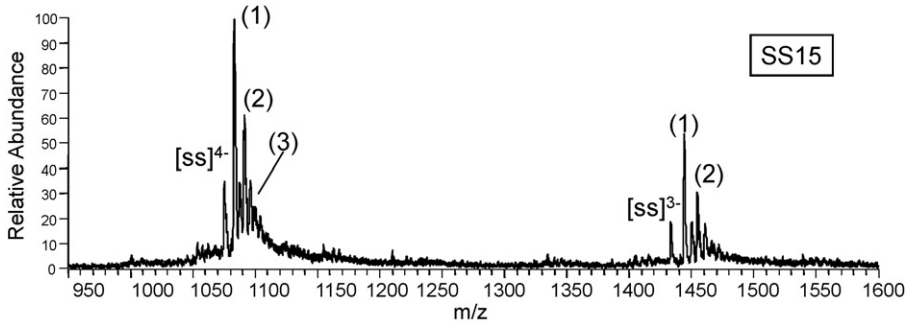

Fig. 4. ESI-mass spectrum showing KMnO4 reactivity with d(GGCGTAGGCATCGC) (SS15). Each ion retaining a KMnO4 adduct is labeled with the number of adducts indicated in parenthesis.

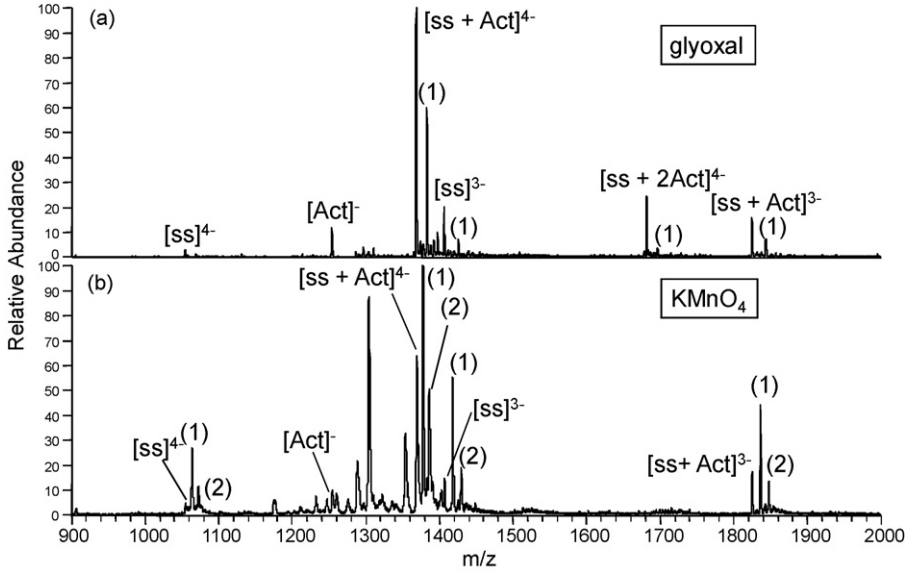

Fig. 5. ESI-mass spectra showing (a) glyoxal and (b) KMnO4 reactivity with actinomycin (Act) complexes of d(GCGATGCCTACGCC) (SS12). Each ion retaining a glyoxal or KMnO4 adduct is labeled with the number of adducts indicated in parenthesis.

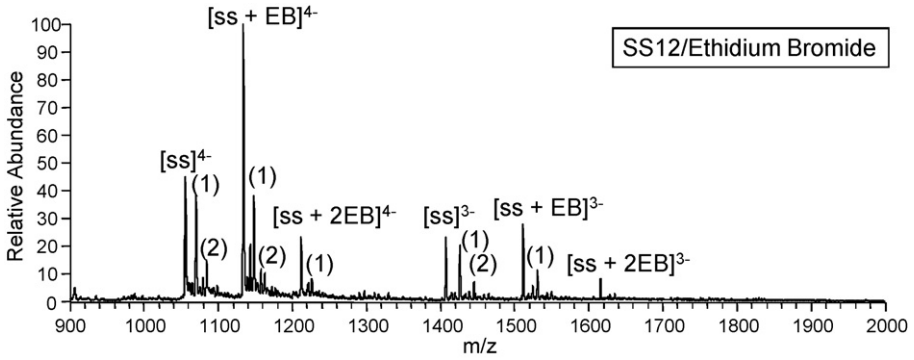

Fig. 6. ESI-mass spectrum showing glyoxal reactivity with d(GCGATGCCTACGCC) (SS12) after ethidium bromide (EB) was bound to the DNA. An ion retaining a glyoxal adduct is labeled with the number of adducts indicated in parenthesis.

3.3. *Reactivity of glyoxal and potassium permanganate with non-covalent DNA/ligand complexes*

The reactivity of both glyoxal and potassium permanganate with non-covalent single strand DNA/ligand complexes was also studied to determine how changes in accessibility of nucleobases caused by ligand binding affect reactivity. Two ligands that are known to bind to single strand DNA were used for this facet of the study. Actinomycin D is thought to interact with single strand oligodeoxynucleotides around GC-rich regions [35,36]. Ethidium bromide, another DNA-interactive agent, has a less specific binding pattern but prior evidence suggests that it also prefers GC sites [37,38]. Our interest focused on elucidating the impact of these ligands on the reactivity of thymines and guanines as monitored by using the two complementary chemical probes in conjunction with ESI-MS. As an example, Fig. 5 shows the product distributions obtained upon reaction of glyoxal or $KMnO_4$ with [d(GCGATGCCTACGCC) (SS12) + actinomycin] complexes. Compared to the high reactivity of glyoxal with free GCGATGCCTACGCC, much lower reactivity is observed for the DNA/actinomycin complexes (Fig. 5a), both in the percent reactivity (i.e. decreasing from 84% to 53% for glyoxal upon actinomycin binding) and the net adduction value (decreasing from 2.2 to 1.0 upon actinomycin binding). A more modest decrease in reactivity is likewise observed for the analogous $KMnO_4$ oxidation reactions (Fig. 5b). The reactivity values are summarized in Table 3. It should be noted that the non-covalent complexes formed between actinomycin or ethidium bromide and DNA are dynamic, in which the ongoing association and dissociation of the complexes means that no particular DNA site is ever completely inaccessible (for reaction with a chemical probe). The product ion abundances measured by ESI-MS represent a snapshot of this dynamic equilibrium, thus depending on both the reactivity of the chemical probes at specific nucleobase sites as well as the binding constants (on and off rates) of the DNA/ligand complexes. To account for differences in the binding constants of the DNA/ligand complexes, the abundances of the products containing the adducted chemical probes are compared to the abundances of products in the absence of the chemical probes with the assumption that the on/off rates for the formation of DNA/ligand complexes remain the same for these comparative experiments (but certainly not the same if using different ligands or different DNA sequences).

Table 3
Glyoxal and $KMnO_4$ reactivity with DNA/ligand complexes.[a].

DNA or DNA complex	% glyoxal reactivity	% $KMnO_4$ reactivity
SS12 5′-GCGATGCCTACGCC-3′	84 ± 13	88 ± 8
SS12 ± 1 actinomycin	53 ± 11	75 ± 8
SS12 ± 2 actinomycin	14 ± 3	na
SS12 ± 1 ethidium bromide	34 ± 12	na
SS12 ± 2 ethidium bromide	15 ± 8	na

[a] The percent reactivities are determined for solutions containing a DNA single strand (40 μM in 50 μL of 90 mM ammonium acetate) incubated with a glyoxal or $KMnO_4$ solution for 30 min at room temperature. The ligand (actinomycin or ethidium bromide) was added at 120 μM and the solution was allowed to equilibrate for at least 30 min at room temperature. The percent reactivity value is a measure of the extent of reaction of the selected DNA or DNA complex (see equation in Section 2) based on relative abundances of reacted and unreacted DNA ions. The net adduction value is a measure of the average number of reactions of the selected DNA or DNA complex (see equation in Section 2).

Actinomycin binding diminishes the formation of the permanganate oxidized products to a lesser extent (i.e. decreasing from 88% to 75% for $KMnO_4$ upon actinomycin binding) as well as the net adduction value (1.6–1.3). We speculate that the more notable decrease observed for the glyoxal reactivity arises from a differential reduction in the accessibility of the targeted nucleobase sites to the two chemical probes. A further decrease in glyoxal reactivity is observed when two actinomycin D ligands are bound. For example, the presence of a second actinomycin ligand decreases the reactivity of the DNA strand with glyoxal from 53% to 28%. The reduction in the glyoxal adduct formation suggests that actinomycin D preferentially binds to the more G-rich regions, thus partially blocking those regions as expected based on prior investigations of the binding sites of this DNA-interactive ligand [36].

The impact of actinomycin binding was further studied using two 8-mer oligodeoxynucleotides, d(CGCGTAAA) and d(CGCGAAAT). Actinomycin is expected to interact with the GC-rich region on the 5′ end of both of these sequences, thus causing a potential decrease in the glyoxal reactivity. However, the $KMnO_4$ reactivity is anticipated to be greater for the second sequence in which the thymine is farther from the putative actinomycin binding region. For the unbound oligodeoxynucleotides, the glyoxal reactivity values were found to be 52% for d(CGCGTAAA) and 38% for d(CGCGAAAT), and the $KMnO_4$ reactivity values were 39% and 43% for the same two sequences. The glyoxal reactivity decreased to 14% and 13%, respectively, when one actinomycin was bound to each of the two sequences, indicating a significant suppression that is attributed to a reduction in the guanine accessibility. The $KMnO_4$ reactivity values decreased to 20% and 27%, respectively, suggesting that the thymine located farther from the GC-rich area remains more accessible to oxidation.

The reactions of single strand oligodeoxynucleotide/ethidium bromide complexes with glyoxal were also evaluated. For these experiments, $KMnO_4$ could not be used to investigate the ethidium bromide complexes because the addition of $KMnO_4$ causes a loss of the ethidium bromide and a degradation of the DNA/ligand complexes [24]. Fig. 6 shows the adduction of glyoxal to the non-covalent d(GCGATGCCTACGCC)/ethidium bromide complexes. The degree of glyoxal adduction to the DNA/ethidium bromide com-

plexes is lower than observed for the native DNA as shown from the reactivity values in Table 3. The glyoxal reactivity of the unbound single strand was 84%, but this value drops to 34% upon binding of ethidium bromide. A notable large decrease in reactivity is observed for the DNA/ethidium bromide complexes, even more so than observed for the analogous DNA/actinomycin complexes. Binding of a second ethidium bromide caused an additional decrease in glyoxal reactivity with the oligodeoxynucleotide (15%), a result expected based on a further loss of guanine accessibility when two molecules of ethidium bromide are associated with the DNA.

4. Conclusions

Glyoxal and $KMnO_4$ are known to be useful chemical probes for determining the orientation of DNA and potential application in determining ligand binding sites. Electrospray ionization mass spectrometry provides a convenient way to monitor the reactions of these chemical probes with DNA because characteristic mass shifts, +58 Da for glyoxal and +34 Da for $KMnO_4$, allow ready tracking of adduct formation. Based on the changes in abundances of the resulting products in the ESI-mass spectra, the high reactivity that is observed for the oligodeoxynucleotides with the chemical probes decreases substantially upon base-pairing in duplexes or once a ligand is bound to the single strands. By comparing the reactivity (as reflected in the product ion abundances) obtained in the presence and absence of a ligand or upon base-pairing, the disruption of nucleobase accessibility can be evaluated systematically. Although glyoxal is known to react with guanine residues, a considerable amount of sequence dependence was also seen upon interaction with DNA. Greater glyoxal reactivity was observed when than the guanine was located on the 5′ end of the oligodeoxynucleotide versus the 3′ end or the center of the sequence. Little or no sequence dependence was observed for analogous reactions with $KMnO_4$. In general, ESI mass spectrometry provides a means to examine specific factors that influence the reactivities of the chemical probes with DNA.

Acknowledgements

Funding from the Robert A. Welch Foundation (F-1155) and the National Institutes of Health (RO1 GM65956) is gratefully acknowledged.

Appendix A. Supplementary data

Supplementary data associated with this article can be found, in the online version, at doi:10.1016/j.ijms.2010.06.007.

References

[1] X. Han, X. Gao, Sequence specific recognition of ligand–DNA complexes studied by NMR, Curr. Med. Chem. 8 (5) (2001) 551–581.
[2] D.R. Boer, A. Canals, M. Coll, DNA-binding drugs caught in action: the latest 3D pictures of drug–DNA complexes, Dalton Trans. 3 (2009) 399–414.
[3] M. Egli, Nucleic acid crystallography: current progress, Curr. Opin. Chem. Biol. 8 (6) (2004) 580–591.
[4] C. Hiort, B. Norden, A. Rodger, Enantiopreferential DNA binding of [ruthenium(II)(1,10-phenanthroline)3]2+ studied with linear and circular dichroism, J. Am. Chem. Soc. 112 (5) (1990) 1971–1982.
[5] D.Z.M. Coggan, I.S. Haworth, P.J. Bates, A. Robinson, A. Rodger, DNA binding of ruthenium tris(1,10-phenanthroline): evidence for the dependence of binding mode on metal complex concentration, Inorg. Chem. 38 (20) (1999) 4486–4497.
[6] A.R. Urbach, M.J. Waring, D.N.A. Visualizing, Footprinting and 1-2D gels, Mol. Biosyst. 1 (4) (2005) 287–293.
[7] C.T. Bui, K. Rees, R.G.H. Cotton, Current chemicals used for probing DNA conformational changes and detection of unknown mutations, Curr. Pharmacogenomics 2 (4) (2004) 325–332.
[8] P.E. Nielsen, Chemical and photochemical probing of DNA complexes, J. Mol. Recognit. 3 (1) (1990) 1–25.
[9] J.T. Millard, Molecular probes of DNA structure, Comp. Nat. Prod. Chem. 7 (1999) 81–103.
[10] A. Bhattacharyya, D.M.J. Lilley, Single base mismatches in DNA. Long- and short-range structure probed by analysis of axis trajectory and local chemical reactivity, J. Mol. Biol. 209 (4) (1989) 583–597.
[11] C. Bailly, Diethylpyrocarbonate and osmium tetroxide as probes for drug-induced changes in DNA conformation in vitro. Methods in Molecular Biology (Totowa, New Jersey) 90 (Drug–DNA Interaction Protocols) (1997) 51–79.
[12] R.G. Cotton, N.R. Rodrigues, R.C. Campbell, Reactivity of cytosine and thymine in single-base-pair mismatches with hydroxylamine and osmium tetroxide and its application to the study of mutations, Prod. Nat. Acad. Sci. 85 (12) (1988) 4397–4401.
[13] K. Usdin, A.V. Furano, The structure of the guanine-rich polypurine:polypyrimidine sequence at the right end of the rat L1 (LINE) element, J. Biol. Chem. 264 (26) (1989) 15681–15687.
[14] M. Buckle, H. Buc, Fine mapping of DNA single-stranded regions using base-specific chemical probes. Study of an open complex formed between RNA polymerase and the lac UV5 promoter, Biochemistry 28 (10) (1989) 4388–4396.
[15] J.G. McCarthy, L.D. Williams, A. Rich, Chemical reactivity of potassium permanganate and diethyl pyrocarbonate with B DNA: specific reactivity with short A-tracts, Biochemistry 29 (25) (1990) 6071–6081.
[16] E.A. Abordo, H. Minhas, P.J. Thornalley, Accumulation of α-oxoaldehydes during oxidative stress: a role in cytotoxicity, Biochem. Pharmacol. 58 (4) (1999) 641–648.
[17] D. Pluskota-Karwatka, A.J. Pawlowicz, M. Tomas, L. Kronberg, Formation of adducts in the reaction of glyoxal with 2′-deoxyguanosine and with calf thymus DNA, Biorg. Chem. 36 (2) (2008) 57–64.
[18] N. Murata-Kamiya, H. Kamiya, H. Kaji, H. Kasai, Mutational specificity of glyoxal, a product of DNA oxidation, in the lacI gene of wild-type Escherichia coli W3110, Mut. Res. Fund. Mol. Mech. Mutagn. 377 (2) (1997) 255–262.
[19] N. Murata-Kamiya, H. Kamiya, H. Kaji, H. Kasai, Glyoxal a major product of DNA oxidation, induces mutations at G:C sites on a shuttle vector plasmid replicated in mammalian cells, Nucleic Acids Res. 25 (10) (1997) 1897–1902.
[20] N. Murata-Kamiya, H. Kaji, H. Kasai, Types of mutations induced by glyoxal, a major oxidative DNA-damage product, in Salmonella typhimurium, Mut. Res. Fund. Mol. Mech. Mutagn. 377 (1) (1997) 13–16.
[21] R. Shapiro, J. Hachmann, The reaction of guanine derivatives with 1,2-dicarbonyl compounds, Biochemistry 5 (9) (1966) 2799–2807.
[22] E. Paleček, P. Boubliková, K. Nejedlý, G. Galazka, J. Klysik, B–Z junctions in supercoiled pRW751 DNA contain unpaired bases or non-Watson–Crick base pairs, J. Biomol. Struct. Dyn. 5 (2) (1987) 297–306.
[23] J.R. Hutton, J.G. Wetmur, Effect of chemical modification on the rate of renaturation of deoxyribonucleic acid. Deaminated and glyoxalated deoxyribonucleic acid, Biochemistry 12 (3) (1973) 558–563.
[24] C.L. Mazzitelli, J.S. Brodbelt, Probing ligand binding to duplex DNA using $KMnO_4$ reactions and electrospray ionization tandem mass spectrometry, Anal. Chem. 79 (12) (2007) 4636–4647.
[25] E. Roberts, V.J. Deeble, C.G. Woods, G.R. Taylor, Potassium permanganate and tetraethylammonium chloride are a safe and effective substitute for osmium tetroxide in solid-phase fluorescent chemical cleavage of mismatch, Nucleic Acids Res. 25 (16) (1997) 3377–3378.
[26] C.T. Bui, K. Rees, R.G.H. Cotton, Permanganate oxidation reactions of DNA: perspective in biological studies, Nucleosides Nucleotides Nucleic Acids 22 (9) (2003) 1835–1855.
[27] S.E. Pierce, R. Kieltyka, H.F. Sleiman, J.S. Brodbelt, Evaluation of binding selectivities and affinities of platinum-based quadruplex interactive complexes by electrospray ionization mass spectrometry, Biopolymers 91 (4) (2009) 233–243.
[28] K.A. Kellersberger, E. Yu, G.H. Kruppa, M.M. Young, D. Fabris, Top-down characterization of nucleic acids modified by structural probes using high-resolution tandem mass spectrometry and automated data interpretation, Anal. Chem. 76 (9) (2004) 2438–2445.
[29] E.T. Yu, Q. Zhang, D. Fabris, Untying the FIV frameshifting pseudoknot structure by MS3D, J. Mol. Biol. 345 (1) (2005) 69–80.
[30] E. Yu, D. Fabris, Toward multiplexing the application of solvent accessibility probes for the investigation of RNA three-dimensional structures by electrospray ionization-Fourier transform mass spectrometry, Anal. Biochem. 334 (2) (2004) 356–366.
[31] E. Yu, D. Fabris, Direct probing of RNA structures and RNA–protein Interactions in the HIV-1 packaging signal by chemical modification and electrospray ionization Fourier transform mass spectrometry, J. Mol. Biol. 330 (2) (2003) 211–223.
[32] K.B. Turner, H.Y. Yi-Brunozzi, R.G. Brinson, J.P. Marino, D. Fabris, S.F. Le Grice, SHAMS: combining chemical modification of RNA with mass spectrometry to examine polypurine tract-containing RNA/DNA hybrids, RNA 15 (8) (2009) 1605–1613.
[33] R.A. Dimitrov, M. Zuker, Prediction of hybridization and melting for double-stranded nucleic acids, Biophys. J. 87 (2004) 215–226.
[34] N.R. Markham, M. Zuker, DINAMelt web server for nucleic acid melting prediction, Nucleic Acid Res. 33 (2005) W577–W581.
[35] Y.L. Hsieh, Y.T. Li, J.D. Henion, B. Ganem, Studies of non-covalent interactions of actinomycin D with single-stranded oligodeoxynucleotides by ion spray mass spectrometry and tandem mass spectrometry, Biol. Mass Spectrom. 23 (5) (1994) 272–276.
[36] H. Yoo, R.L. Rill, Actinomycin, D binding to unstructured, single-stranded DNA, J. Mol. Recognit. 14 (3) (2001) 145–150.

[37] D.B. Davies, S.F. Baranovsky, A.N. Veselkov, Structural and thermodynamical analysis of drug binding to single-stranded DNA oligomers. Self-association of non-self-complementary deoxytetranucleotides of different base sequence and their complexation with ethidium bromide in aqueous solution, J. Chem. Soc. Faraday Trans. 93 (8) (1997) 1559–1572.

[38] D.B. Davies, L.N. Djimant, S.F. Baranovsky, A.N. Veselkov, 1H-NMR determination of the thermodynamics of drug complexation with single-stranded and double-stranded oligodeoxynucleotides in solution: ethidium bromide complexation with the deoxytetranucleotides 5′-d(ApCpGpT), 5′-d(ApGpCpT), and 5′-d(TpGpCpA), Biopolymers 42 (3) (1997) 285–295.